Magnetic properties of MoS_2: Existence of ferromagnetism

Sefaattin Tongay,[1,2,a),b)] Sima S. Varnoosfaderani,[3,b)] Bill R. Appleton,[2,4] Junqiao Wu,[1] and Arthur F. Hebard[3,a),b)]
[1]*Department of Materials Science and Engineering, University of California, Berkeley, California 94720, USA*
[2]*Department of Materials Science and Engineering, University of Florida, Gainesville, Florida 32611, USA*
[3]*Department of Physics, University of Florida, Gainesville, Florida 32611, USA*
[4]*Nanoscience Institute for Medical and Engineering Technology, University of Florida, Gainesville, Florida 32611, USA*

(Received 27 May 2012; accepted 4 September 2012; published online 18 September 2012)

We report on the magnetic properties of MoS_2 measured from room temperature down to 10 K and magnetic fields up to 5 T. We find that single crystals of MoS_2 display ferromagnetism superimposed onto large temperature-dependent diamagnetism and have observed that ferromagnetism persists from 10 K up to room temperature. We attribute the existence of ferromagnetism partly to the presence of zigzag edges in the magnetic ground state at the grain boundaries. Since the magnetic measurements are relatively insensitive to the interlayer coupling, these results are expected to be valid in the single layer limit. © *2012 American Institute of Physics*. [http://dx.doi.org/10.1063/1.4753797]

After graphene became experimentally accessible,[1] it has become a popular choice for various kinds of applications such as diodes,[2,3] solar cells,[4] and high-frequency[5] devices owing to its extraordinary properties. While zero-band gap graphene is one of the most studied two-dimensional (2D) materials, other finite band gap 2D materials provide an extended range of applications. To this end, layered transition metal dichalcogenides (TMDs) offer numerous kinds of 2D materials with different physical properties. MoS_2 is one of the most stable layered TMDs, naturally occurring in nature, and consists of covalently bonded three hexagonal atomic layers (S-Mo-S) enabling formation of 2D layers. The interlayer separation is ~6.2 Å and therefore the Van der Waals forces between the adjacent layers are very weak and individual layers can be isolated using traditional mechanical cleavage techniques. More recently, molybdenum disulfide (MoS_2) has received considerable attention because of the possibility of synthesizing large area atomically thin semiconducting sheets having relatively large in-plane mobility,[6,7] mechanical stability,[8,9] and ideal band gap (E_g) values ranging from 1.3 eV (indirect) in bulk limit to 1.8 eV (direct) for isolated MoS_2 layers. So far, MoS_2 has been explored in diverse fields and integrated in transistors,[7] sensors,[10] and used as a solid state lubricant and catalyst for hydrodesulfurization and hydrogen evolution.[11]

Even though the electrical,[12,13] mechanical,[9] and optical properties[14–17] of MoS_2 have been studied both theoretically and experimentally, recent studies on the magnetic response of MoS_2 are limited to theoretical calculations.[8,9,18,19] According to these calculations, edges with different directions of termination remain in different magnetic ground states. While the armchair edges are stable in a non-magnetic (or meta-stable magnetic[18] state, the zigzag edges are in a magnetic ground state[8,18] with a net magnetic moment. From this point of view, in the presence of zigzag edges, magnetism should be observed in MoS_2 nanoribbons, nanocrystalline thin films, and even in bulk limit provided that the average grain size is small enough.

Here, we study the magnetic properties of MoS_2 experimentally from 300 K down to 10 K and from 0 to 5 T. Our results suggest that the magnetization of MoS_2 comprises two main terms in the bulk limit: (1) a temperature-dependent diamagnetic background and (2) ferromagnetism possibly originating from existence of zigzag edges with associated magnetism at grain boundaries. A full understanding of the magnetic properties of MoS_2 is crucial for the successful integration of MoS_2 into possible devices.

Commercially available (SPI supplies) MoS_2 and home-grown single crystals (see Figs. 1(a) and 1(b)) have been measured from room temperature down to 10 K using a superconducting quantum interference device (SQUID) up to 5 T. Prior to the magnetization measurements, samples have been carefully cleaned using organic solvents and then have been characterized using 532 nm Raman spectroscopy, x-ray photoelectron spectroscopy (XPS), and x-ray diffraction (XRD). Typical sample size was a few millimeters in the in-plane direction and 10–100 μm in thickness (c-axis). Fig. 2(a) shows Raman spectra taken on the MoS_2 surface (blue) and at the grain boundaries (red). The peaks located at ~378 cm^{-1} and ~402 cm^{-1} are identified as E^1_{2g} and A_{1g} modes which are associated with vibrations of Mo and S atoms in the basal plane and only S along the c-axis respectively.

While the E^1_{2g} and A_{1g} modes are observed both on the surface and at the grain boundaries, these modes do not display any significant differences in peak position or height. However, we note that an additional peak develops at ~282 cm^{-1} only on the grain boundaries which can be attributed to the E_{1g} mode. In principle, the latter mode is forbidden when the sample is oriented with the surface normal of the basal layers pointed in the opposite direction to the incoming laser, therefore, enhancement in the E_{1g} peak is related to the misorientation of the basal planes.

The XPS spectra taken on the MoS_2 (Fig. 2(b)) show characteristic Mo and S peaks (~1:2 elemental ratio)

a)Authors to whom correspondence should be addressed. Electronic addresses: tongay@berkeley.edu and afh@phys.ufl.edu.
b)S. Tongay, A. F. Hebard, and S. S. Varnoosfaderani contributed equally to this work.

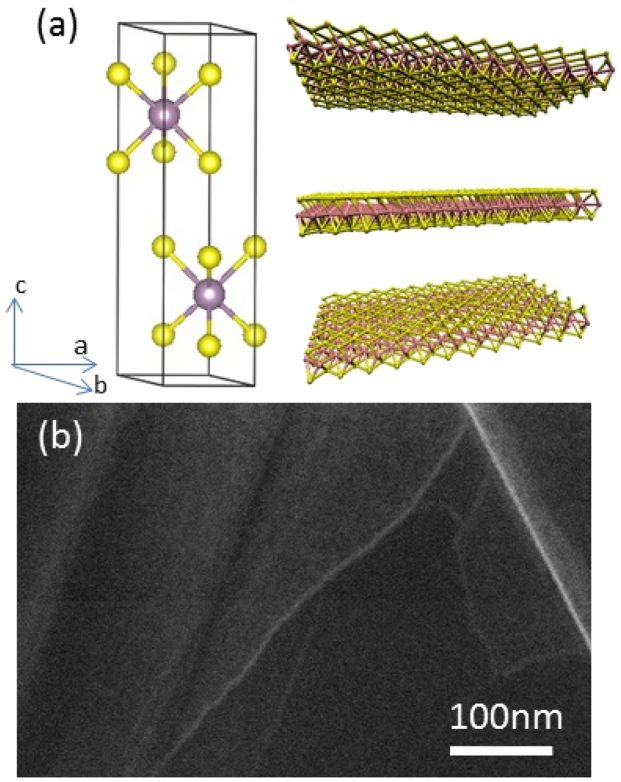

FIG. 1. (a) Unit cell of MoS_2 and the layered view of the crystal. (b) Typical scanning electron image taken on the MoS_2 surface.

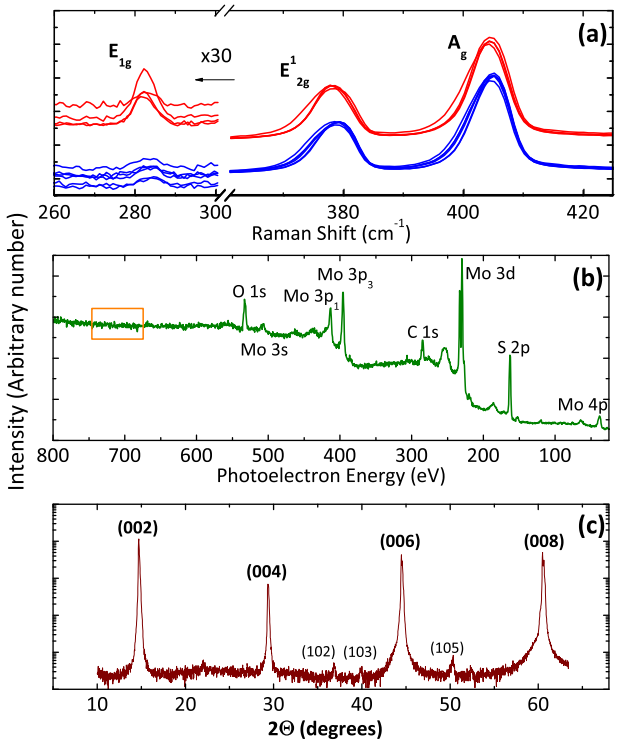

FIG. 2. (a) Raman spectrum taken on the surface (blue) and at the grain boundaries (red) of MoS_2. (b) XPS spectrum and (c) XRD pattern taken on MoS_2 surface.

without any significant magnetic impurity (Fig. 2(b) orange rectangle). The observed O and C peaks are due to interaction with air and carbon contamination on the surface.

XRD data (Fig. 2(c)) show (002) and higher order Bragg peaks implying that the MoS_2 planes are preferentially oriented in the (002) direction. Other minor directions, such as (102), (103), and (105) also exist in the crystal. Using the Scherrer equation and the FWHM value of the (002) peak, we estimate the average crystallite size around 76 nm. We note that the instrumental broadening for our instrument is much smaller than the observed FWHM for (002) peak, and therefore the average crystallite size estimate is valid. We further confirm the small grain sizes from the scanning electron microscopy measurements (Fig. 1(b)), however, we note that grains that are larger than 100 nm have also been observed from sample to sample.

In principle, single crystals of semiconducting MoS_2 are expected to be diamagnetic just like any other semiconductor. Even though the magnetic response is dominated by diamagnetism as shown in Fig. 3(a), we find that the diamagnetic background is superimposed onto the ferromagnetic loop (Fig. 3(b)) implying that the total magnetic susceptibility comprises both diamagnetic and ferromagnetic parts. In layered materials such as graphite, χ_{dia} depends on the direction of the applied field with respect to the c-axis: when the field is parallel to the c-axis ($\chi_{dia}^{\parallel}$), electrons' contribution to the diamagnetism is optimized and in the perpendicular direction ($\chi_{dia}^{\perp}$), electrons are localized and their contribution is mostly limited to the core diamagnetism. Using linear regression in the high field range, we find that the parallel diamagnetic susceptibility, $\chi_{dia}^{\parallel} = \mathrm{M(H)/H}$, is around 1×10^{-6} emu/g with a magnetic anisotropy ($\chi_{dia}^{\parallel}/\chi_{dia}^{\perp}$) in the range 1.2–1.5. We also note that the magnetic response is similar in both the parallel and perpendicular directions.

The ferromagnetic component in MoS_2 is determined after subtracting out the diamagnetic part. In Fig. 3(c), the ferromagnetic response at different temperatures has been plotted with respect to the magnetic field applied parallel to the c-axis. We first observe that saturation magnetization (M_s) remains unchanged with respect to the temperature while the coercive field (H_r) slightly increases from 100 Oe to 400 Oe which is small comparing to the field range where the ferromagnetic hysteresis is observed. Even though the observed ferromagnetism in MoS_2 is in the bulk limit, previous work has shown that MoS_2 nanoplates grown by RF sputtering display large ferromagnetic behavior[20] and this effect has been attributed to the existence of the zigzag edges in the ferromagnetic ground state. More recently, various theoretical calculations predicted ferromagnetism in MoS_2 in the presence of zigzag edges[8,9,18] and sulfur vacancies.[19] The net magnetic moment arising from these zigzag edges is expected to decrease with increasing grain size (or ribbon width), and therefore the ferromagnetic signal becomes negligible in the bulk limit. However, since the average grain size in the MoS_2 samples is around ~75 nm, in reality measured MoS_2 samples contain significant amount of grain boundaries with arbitrary distribution of zigzag and armchair edges that are likely to yield enough ferromagnetic signal.[8] Using the optimized MoS_2 lattice constants, the average μ_b per MoS_2,[8] and the average grain size extracted from XRD measurements, we estimate the ferromagnetic signal originating from zigzag edges to be around 2.6×10^{-2} emu/g.

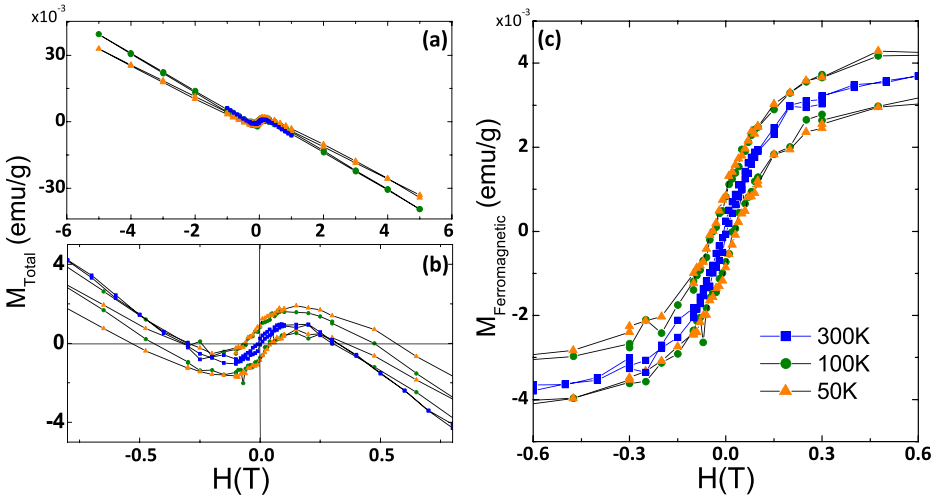

FIG. 3. (a) Magnetization (M) vs applied field (H) data taken at different temperatures in the field parallel to the c-axis direction. (b) M-H curves displayed at lower magnetic fields. (c) $M_{ferromagnetic}$ vs H curves after subtracting out the diamagnetic background.

Here, we note that the zigzag edges are chemically more stable and energetically favorable[8,9] compared to the armchair configuration, and under the assumption that zigzag edges are only 10% of the grain boundary, the total magnetization value still remains on the same order of magnitude with our measured saturated moment of $\sim 4 \times 10^{-3}$ emu/g (Fig. 3(c)).

Moreover, other effects such as coupling between the adjacent sheets are known to stabilize the magnetism and can enhance the total magnetization originating from the grain boundaries. The latter effect has been observed in other non-magnetic layered system, graphite, at the grain boundaries where the ferromagnetic signal was attributed to localized electronic states at grain boundaries.[21] Even though, the interlayer coupling might be enhancing the ferromagnetic signal, such coupling is not a necessary condition for the existence of ferromagnetism as the presence of zigzag edges is sufficient.[8,9,18] In this sense, magnetization measurements certainly probe the contribution from zigzag edges (single layer behavior) while the ferromagnetic contribution from coupling of these edges is neither necessary nor guaranteed. An interesting way to test the effect of interlayer coupling which warrants future studies would be to intercalate non-magnetic species so as to further reduce the interlayer coupling.

Although the above discussions convincingly present the possibility of ferromagnetism originating from the zigzag edges, another common cause for the observed ferromagnetism might be related to the existence of magnetic impurities in the sample. As XPS spectra taken on MoS_2 surfaces show, there is no sign of magnetic impurities in the region where the magnetic impurity peaks are present (Fig. 2(b) orange box), yet some impurities beyond the detection limit might be partially contributing to the total magnetization and can not be ruled out. Here, we note that the XPS instrument used in this study has 0.005%-0.01% sensitivity in the multiplex mode and even if there are magnetic impurities within the detection limit that are clustered enough to induce ferromagnetism, this alone cannot account for the observed ferromagnetic behavior. Lastly, one would expect the saturation magnetization to be temperature dependent with negligible coersive field values[22] in contrast to what has been observed in our measurements (Fig. 3(c)). Despite intense research, the origin of the ferromagnetism in the similar 2D system, graphite, remains controversial even after a decade. Since the MoS_2 and graphite share similar properties (i.e., existence of magnetism at zigzag edges), we believe that magnetic properties of MoS_2 are likely to will remain somewhat controversial and the presence of ferromagnetism should be taken with care.

A more detailed examination of the diamagnetic properties is shown in Fig. 4(a) (blue diamonds) where the temperature dependence of $\chi_{\parallel}^{dia}$ is plotted. The susceptibilities were determined from the slope of $M(H)$ curves taken at specific temperatures. In general, semiconductors exhibit temperature-independent diamagnetic behavior as opposed to the temperature-dependent behavior observed in Fig. 4(a). Plotting the diamagnetic susceptibility as a function of $1000/T^{-1}$, we find that the diamagnetic susceptibility scales linearly with inverse temperature from 300 K down to 20 K. This behavior can be attributed to Curie paramagnetism which emerges in the presence of localized unpaired spin

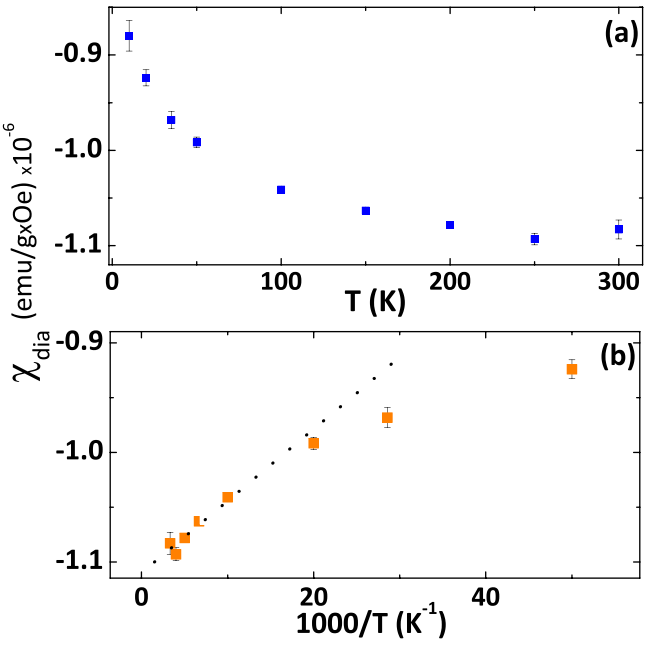

FIG. 4. (a) Diamagnetic susceptibility vs temperature (b) Diamagnetic susceptibility vs 1000/T plots displaying the 1/T behavior.

states (paramagnetic states) that might be associated with the dangling bonds at the grain boundaries, vacancies, and localized edge states.[23,24] The observed linearity breaks down below 20 K (Fig. 4(a)) possibly due to the antiferromagnetic exchange interaction between the unpaired spin states enabled at low temperatures.[23]

In conclusion, we have studied the magnetic properties of single crystal MoS_2 in the bulk limit and have presented results which show that the magnetic response comprises both diamagnetic and the ferromagnetic terms. The observed ferromagnetism is interesting and unexpected since the MoS_2 crystals are non-magnetic. We partly attribute the existence of ferromagnetism to the presence of zigzag edges within the grain boundaries in the magnetic ground state as predicted by recent density functional theory calculations.[8,9,18] Magnetic impurities, and magnetism from sulfur vacancies[19] might be other factors contributing to the total ferromagnetic signal. We also note that since the magnetic measurements are insensitive to the interlayer coupling, the presented results are valid in the single layer MoS_2 limit.

This work is supported by the Office of Naval Research (ONR) under Contract No. 00075094 (B.R.A.) and by the National Science Foundation (NSF) under Contract No. 1005301 (A.F.H.).

[1]K. S. Novoselov, A. K. Geim, S. V. Morozov, D. Jiang, Y. Zhang, S. V. Dubonos, I. V. Grigorieva, and A. A. Firsov, Science **306**, 666–669 (2004).
[2]S. Tongay, M. Lemaitre, X. Miao, B. Gila, B. R. Appleton, and A. F. Hebard, Phys. Rev. X **2**, 011002 (2012).
[3]S. Tongay, M. Lemaitre, T. Schumann, K. Berke, B. R. Appleton, B. Gila, and A. F. Hebard, Appl. Phys. Lett. **99**, 102102 (2011).
[4]X. Miao, S. Tongay, M. K. Petterson, K. Berke, A. G. Rinzler, B. R. Appleton, and A. F. Hebard, Nano Lett. **12**, 2745–2750 (2012).
[5]Y. Wu, Y.-M. Lin, A. A. Bol, K. A. Jenkins, F. Xia, D. B. Farmer, Y. Zhu, and P. Avouris, Nature **472**, 74–78 (2011).
[6]R. Fivaz and E. Mooser, Phys. Rev. **163**, 743–755 (1967).
[7]B. Radisavljevic, A. Radenovic, J. Brivio, V. Giacometti, and A. Kis, Nat. Nanotechnol. **6**, 147–150 (2011).
[8]Y. Li, Z. Zhou, S. Zhang, and Z. Chen, J. Am. Chem. Soc. **130**, 16739–16744 (2008).
[9]C. Ataca, H. Sahin, E. Akturk, and S. Ciraci, J. Phys. Chem. C **115**, 3934–3941 (2011).
[10]H. Li, Z. Yin, Q. He, H. Li, X. Huang, G. Lu, D. W. H. Fam, A. I. Y. Tok, Q. Zhang, and H. Zhang, Small **8**, 63–67 (2012).
[11]E. Furimsky, Catal. Rev. **22**, 371–400 (1980).
[12]S. H. El-Mahalawy and B. L. Evans, Phys. Status Solidi B **79**, 713–722 (1977).
[13]O. El Beqqali, I. Zorkani, F. Rogemond, H. Chermette, R. B. Chaabane, M. Gamoudi, and G. Guillaud, Synth. Met. **90**, 165–172 (1997).
[14]J. P. Wilcoxon, P. P. Newcomer, and G. A. Samara, J. Appl. Phys. **81**, 7934–7944 (1997).
[15]G. Eda, H. Yamaguchi, D. Voiry, T. Fujita, M. Chen, and M. Chhowalla, Nano Lett. **11**, 5111–5116 (2011).
[16]A. Splendiani, L. Sun, Y. Zhang, T. Li, J. Kim, C.-Y. Chim, G. Galli, and F. Wang, Nano Lett. **10**, 1271–1275 (2010).
[17]T. Korn, S. Heydrich, M. Hirmer, J. Schmutzler, and C. Schüller, Appl. Phys. Lett. **99**, 102109 (2011).
[18]M. Terrones A. R. Botello-Mndez, F. Lopez-Uras, and H. Terrones, Nanotechnology **20**, 325703 (2009).
[19]R. Shidpour, Nanoscale **2**, 1429 (2010).
[20]J. Zhang, J. M. Soon, K. P. Loh, J. Yin, J. Ding, M. B. Sullivian, and P. Wu, Nano Lett. **7**, 2370–2376 (2007).
[21]J. Cervenka, M. I. Katsnelson, and C. F. J. Flipse, Nat. Phys. **5**, 840 (2009).
[22]P. Esquinazi, A. Setzer, R. Höhne, C. Semmelhack, Y. Kopelevich, D. Spemann, T. Butz, B. Kohlstrunk, and M. Lösche, Phys. Rev. B **66**, 024429 (2002).
[23]F. J. Di Salvo, B. G. Bagley, R. S. Hutton, and A. H. Clark, Solid State Commun. **19**, 97–100 (1976).
[24]N. T. Bagraev, L. N. Blinov, and V. V. Romanov, Solid State Commun. **121**, 417–421 (2002).